Applied Catalysis B: Environmental 160–161 (2014) 722–729

Contents lists available at ScienceDirect

Applied Catalysis B: Environmental

journal homepage: www.elsevier.com/locate/apcatb

Dominated factors for high performance of Fe^{3+} grafted metal doped TiO_2 based photocatalysts

Masami Nishikawa[a,*], Ryota Takanami[a], Fumie Nakagoshi[a], Hiroshi Suizu[b], Hideyuki Nagai[b], Yoshio Nosaka[a]

[a] Nagaoka University of Technology, Department of Materials Science and Technology, 1603-1 Kamitomioka, Nagaoka 940-2188, Japan
[b] Mitsui Chemicals Inc., Process Technology Center, 580-32 Nagaura, Sodegaura 299-0265, Japan

ARTICLE INFO

Article history:
Received 7 March 2014
Received in revised form 7 May 2014
Accepted 11 May 2014
Available online 16 May 2014

Keywords:
Titanium dioxide
Photocatalytic reaction mechanism
Fe grafting
Metal doping
Oxygen vacancy

ABSTRACT

We examined dominated factors for visible light driven performance of the Fe^{3+} grafted metal doped TiO_2 based photocatalyst ($Fe/Me:TiO_2$) by means of ESR spectroscopy and active oxygen detection. For the performance of the $Fe/Me:TiO_2$, in addition to a direct electron transfer from TiO_2 valence band to the grafted Fe^{3+}, indirect electron transfers to the Fe^{3+} are important. In this work, it was revealed that the electron acceptor state formed close to the redox potential of the grafted Fe^{3+} to Fe^{2+} by doping metal ions leaded to enhancement of the photocatalytic activity because the efficiency of the indirect electron transfer via acceptor level to the Fe^{3+} was high. The other indirect electron transfer via metal ions of donor state to the Fe^{3+} did not lead to large enhancement of photocatalytic activity. A two-step electron excitation from TiO_2 valence band to conduction band via defect level under visible light irradiation was a path with high recombination rate of electron–hole and therefore could not contribute to the photocatalytic activity. Moreover the defect level decreased the efficiency of the direct electron transfer from the TiO_2 valence band to the Fe^{3+}, resulting in decrease of photocatalytic activity.

1. Introduction

Photocatalysts have attracted much attention in view of their practical application to air and water purifications [1–3]. TiO_2 is one of the most attractive materials because it is inexpensive, easily available and nontoxic. But its bandgaps are 3.2 and 3.0 eV in anatase and rutile forms, respectively, resulting in only the UV light response. Since visible light response is required to effectively utilize indoor light for cleanup of the indoor environments, various modification processes of TiO_2 have been reported to develop the visible light response [4–8].

Among the modification processes of TiO_2 for developing visible light response, the grafting of Fe^{3+} on the TiO_2 surface was one of the promising processes because Fe^{3+} grafted TiO_2 (Fe/TiO_2) was reported to show highest quantum efficiency under visible light irradiation [9]. Fe^{3+} was grafted as an amorphous FeOOH cluster on the surface of TiO_2. We revealed that electron transfer from valence band of TiO_2 to the grafted Fe^{3+} occurred using electron spin resonance (ESR) spectroscopy [10]. This direct electron transfer was origin of visible light response. Furthermore, by chemiluminescence photometry with luminol, we revealed that the Fe^{2+} formed by receiving an electron returned to Fe^{3+} by reduction of O_2 into H_2O_2 by two-electron process. Then, by doping Ru ions into the TiO_2 lattice, after grafting of Fe^{3+} its photocatalytic activity was further enhanced under visible light irradiation. We also reported using ESR spectroscopy that the enhancement would be caused by two kinds of indirect electron transfer to the Fe^{3+} in addition to the direct electron transfer to the Fe^{3+}. One indirect electron transfer was that an electron is photoexcited from valence band to the doped Ru^{4+} and then transfers to the grafted Fe^{3+}. The other indirect electron transfer was that an electron is photoexcited from valence band to conduction band by two-step excitation process via defect level of oxygen vacancy and then transferred to the grafted Fe^{3+}. However, it has been not clear yet which indirect electron transfer to the Fe^{3+}, through the two-step excitation via the defect level or through the doped metal ions, dominates the performance of the Fe^{3+} grafted Ru-doped TiO_2 ($Fe/Ru:TiO_2$) [10].

In addition, for dopants, there are two states; one is donor state and the other is acceptor state. In the case of Rh doped TiO_2 for O_2 evolution from aqueous solution containing Ag^+ ions under visible light irradiation, formation of Rh^{3+} by codoping Sb^{5+} was important

* Corresponding author. Tel.: +81 258 47 9831.
E-mail addresses: nishikawa@vos.nagaokaut.ac.jp, nishikawa@yahoo.co.jp (M. Nishikawa).

http://dx.doi.org/10.1016/j.apcatb.2014.05.020
0926-3373/

for high performance of O_2 evolution [11]. The Rh^{3+} gave an electron to TiO_2 conduction band, i.e., played a role as donor [12]. In contrast, Rh^{4+} which was formed without codoping Sb^{5+} decreased the performance of O_2 evolution. In the case of $SrTiO_3$, Rh^{4+} was reported to be acceptor state [13,14]. Therefore, it was considered that the Rh^{4+} in TiO_2 host played a role as acceptor like the $SrTiO_3$ case. Such states of metal ions, donor or acceptor, significantly affected the O_2 evolution. However, until now, it has been not clear how much donor or acceptor states of dopants affect photocatalytic decomposition performance for gaseous pollutants. Particularly to develop the visible light response of the Fe/TiO_2 based photocatalyst, it is important to determine which indirect electron transfer is more effective, from donor metal ions to conduction band and then to the Fe^{3+} or from valence band to acceptor metal ions and then to the Fe^{3+}. Furthermore, there are metal ions with various redox potentials. Then it has been not also clear how much the redox potential of metal ion affect the indirect electron transfer to the Fe^{3+}.

In this work, to increase the visible light driven photocatalytic activity of the Fe/TiO_2 based photocatalyst, dominated factors for the efficiency of the indirect electron transfer to the Fe^{3+}, i.e., the effects of defect level due to oxygen vacancy, donor or acceptor states of doped metal ions, and the redox potential of doped metal ions on the photocatalytic activity, were clarified.

2. Experimental

2.1. Materials

To examine the effect of oxygen vacancy, TiO_2 (MT-150A, TAYCA) was heated at 500 °C in air or in N_2 atmosphere for 1 h. For doping Rh and Sb ions to examine the effects of donor or acceptor states of Rh ions, $RhCl_3$ and Sb_2O_3 and TiO_2 (FP-6, Showa Titanium Inc.), in which $RhCl_3$ was weighted so that content of Rh ion was 0.01 wt% relative to TiO_2 and Sb_2O_3 was weight so that content of Sb ion was the same as or twice of that of Rh ions, was mixed well and then calcined at 750 °C for 3 h in air. For doping Ru, Rh, Ir and Cr ions to examined the effects of redox potential of metal ion, distilled water was added to a mixture of each metal chloride and TiO_2 (FP-6, Showa Titanium Inc.) in which each metal chloride was weighted so that content of each metal ion was 0.01 wt% relative to TiO_2. Each solution was stirred for 24 h, dried and then calcined at 750 °C for 3 h in air. For comparison, non-doped TiO_2 was also calcined at 750 °C for 3 h in air. The grafting procedure of Fe^{3+} was the same to that reported by Yu et al. [9]. That is, distilled water was added to a mixture of $FeCl_3·6H_2O$ and TiO_2 in which $FeCl_3·6H_2O$ was weighted so that the weight fraction of Fe ion was 0.05 wt% relative to TiO_2. The pH of the solution was adjusted to 2 by adding HCl and then the solution was heated at 90 °C for 1 h under stirring. The obtained photocatalyst was washed with distilled water and then dried at 110 °C for 24 h. Specific surface areas of the obtained photocatalysts using BET method were 4.5–7.6 m^2/g.

2.2. Photocatalytic activity

The photocatalytic activity was measured for the decomposition of gaseous acetaldehyde as follows. Photocatalyst powder of 0.02 g was spread on a Petri dish of 4 cm diameter and then the dish was placed in the circulated reactor with a volume of 260 mL which was filled with mixed gas of O_2/N_2 = 1:4. The acetaldehyde gas of 50 μL and water of 10 mL were injected into the reactor. The dish placed in the reactor was irradiated by a set of LED (light emitting diode) of λ = 470 or 625 nm at the intensity of about 20 mW/cm^2, and the amount of generated CO_2 was monitored by a gas analyzer (LI-COR, LI-840) equipped in the circulation reactor system.

2.3. Electron spin resonance spectroscopy

For ESR measurements, the photocatalyst powder of 20 mg was placed in a quartz glass sample tube with a Young vacuum joint and a stopcock, and then it was evacuated using a rotary pump. The measurement was performed at 77 K with an ESR spectrometer (Bruker, ESP-300E) under irradiation with a 500 W mercury lamp equipped with sharp-cut filters of <620 nm, <560 nm (HOYA, R62 and O56). The microwave frequency was 9.15 GHz (X-band) and the microwave power was fixed at 2 mW. The field modulation was 0.2 mT.

2.4. Luminol chemiluminescence probe methods

The generation of O_2^- was observed by using a luminol chemiluminescence probe method. Photocatalyst of 15 mg was added in 0.01 M NaOH solution of 3.5 mL in a quartz cell (1 cm × 1 cm) and then the suspension was irradiated by a set of LED of λ = 625 nm. After the irradiation, 50 μL of 7 mM luminol solution was

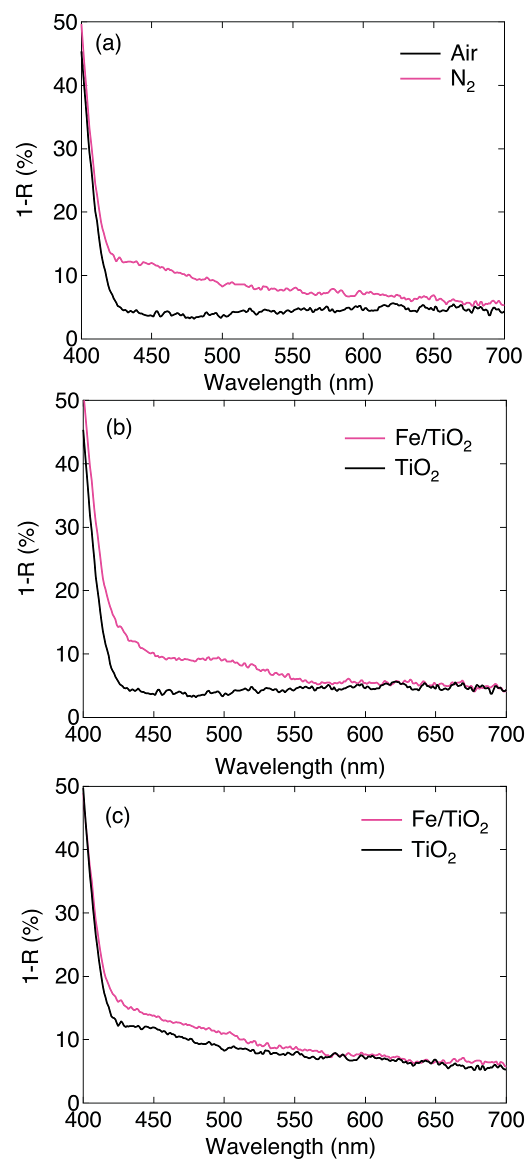

Fig. 1. UV–vis diffuse reflectance spectra of (a) TiO_2 heated at 500 °C in air or N_2 atmosphere for 1 h, (b) TiO_2 treated in air before and after grafting of Fe^{3+} and (c) TiO_2 treated in N_2 before and after grafting of Fe^{3+}.

immediately added in the suspension. The chemiluminescence intensity was measured using a Peltier-cooled photon-counter head (Hamamatsu Photonics, H7421). For the measurements of H_2O_2, the photocatalyst suspension was irradiated by the LED and then was kept in dark to eliminate O_2^-. 50 μL of 7 mM luminol solution was added in the suspension and then the suspension was kept in dark for 10 min. 50 μL of hemoglobin (Hb) solution was added in the suspension and then the chemiluminescence intensity was measured using the Peltier-cooled photon counter head.

To convert the chemiluminescence intensities to the absolute concentration of O_2^- and H_2O_2, the apparatus factor was calculated from the experiment where all luminol molecules are consumed for the reaction with an excess amount of H_2O_2. The integrated number of photons was proportional to the luminol concentration. From the slope, the observed chemiluminescence intensity can be converted to H_2O_2 concentration as mentioned in detail in the previous report [15].

3. Results and discussion

3.1. The effect of defect level due to oxygen vacancy

To clarify which indirect electron transfer to Fe^{3+} via doped metal level or defect level is dominated for high performance of Fe/TiO_2 photocatalyst, the effect of defect level due to oxygen vacancy was examined. Fig. 1 shows UV–vis diffuse reflectance spectra of TiO_2 (MT-150A) heated at 500 °C in air or N_2 atmosphere for 1 h before and after grafting of Fe^{3+}. The absorbance intensity of the TiO_2 treated in N_2 increased at the range of longer wavelength than the absorption due to bandgap excitation. This shows that a large amount of oxygen vacancies were introduced into the TiO_2 lattice by N_2 treatment compared to that treated in air. After grafting of Fe^{3+}, new absorption due to the direct electron transfer from TiO_2 valence band to the Fe^{3+} appeared near the adsorption edge for the TiO_2 treated in air. For the TiO_2 treated in N_2, increment in the absorption intensity due to the direct electron transfer was smaller than that of TiO_2 treated in air. This indicates that the efficiency of the direct electron transfer from TiO_2 valence band to the Fe^{3+} became lowered.

Fig. 2 shows ESR spectra for the TiO_2 treated in air and N_2 measured under dark and light irradiation at 77 K. The TiO_2 treated in air (Fig. 2(a)) showed signals of electrons trapped as Ti^{3+} (g = 1.97) and holes trapped as O^- (g = 2.01) [16,17] even under visible light irradiation. This indicated that the defect level due to oxygen vacancy would be formed in its bandbap. The defect level was reported to be formed below the conduction band by 0.7 eV [18]. From the ESR measurement, under visible light irradiation of $\lambda > 620$ nm the trapped electrons alone were observed. Then under light irradiation of shorter wavelength than 620 nm, the trapped electrons and holes were observed. These results indicates that excitation of electrons trapped at defect level to conduction band would occur under visible light irradiation of $\lambda > 620$ nm, corresponding with <2 eV in photon energy, and then under visible light irradiation of $\lambda < 620$ nm, the two-step electron excitation from valence band to conduction band via the defect level would occur because energy difference between the valence band and the defect level is about 2.3 eV. Therefore, the TiO_2 treated in air seemed to have oxygen vacancy to some extent.

For the TiO_2 treated in N_2 (Fig. 2(b)), under visible light irradiation of $\lambda > 620$ nm, trapped electrons alone were observed and under visible light irradiation of $\lambda < 620$ nm, trapped electrons and holes were observed like the case of the TiO_2 treated in air. The

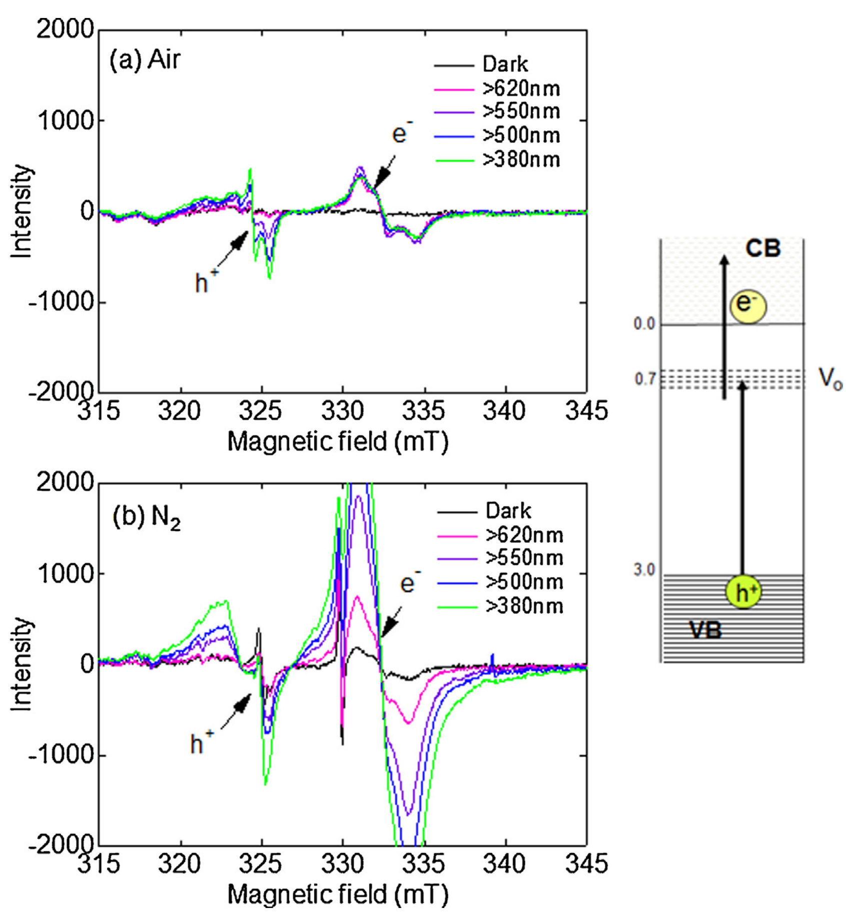

Fig. 2. ESR spectra of TiO_2 treated in (a) air and (b) N_2under dark and light irradiation at 77 K.

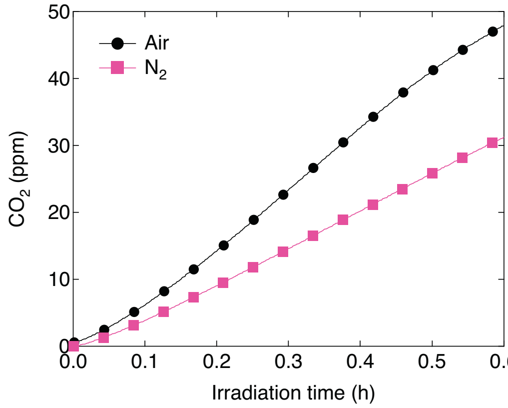

Fig. 3. Time profiles of CO_2 generated by photocatalytic decomposition of gaseous acetaldehyde on the Fe/TiO_2 under visible light irradiation ($\lambda = 470$).

signal intensities of the trapped electrons and holes became much larger than those in the TiO_2 treated in air. Therefore, by treating in N_2 a large amount of oxygen vacancies were introduced in the TiO_2 lattice, leading to active electron excitation from the defect level to conduction band and active two-step electron excitation from valence band to conduction band via the defect level. In the presence of a large amount of oxygen vacancies, the efficiency of the direct electron transfer from TiO_2 valence band to the Fe^{3+} would be largely decreased because the two-step electron excitation via defect level preferentially occurred compared to the direct electron transfer.

After grafting of Fe^{3+} photocatalytic activity under visible light irradiation of $\lambda = 470$ nm-LED was measured. Fig. 3 shows time profiles of CO_2 generated by photocatalytic decomposition of gaseous acetaldehyde on the Fe^{3+} grafted heat treated TiO_2. The photocatalytic activity of TiO_2 treated in N_2 became lower than that of TiO_2 treated in air in spite of the active electron excitation observed in the ESR measurement. This discrepancy would be due to difference in measurement temperature. The ESR measurement was done at 77 K to prolong lifetimes of trapped electron and hole because at room temperature trapped electron and hole could not be observed owing to higher probability of electron–hole recombination with temperature. Then, the trapped electrons and holes observed at 77 K did not contribute to the photocatalytic reaction at room temperature because they were vanished by the recombination before reductive or oxidative reactions.

Therefore, it is revealed that the indirect electron transfer to the Fe^{3+} through the two-step excitation via the defect level is difficult to occur. Furthermore, since oxygen vacancy reduced the efficiency of the direct electron transfer from TiO_2 valence band to the Fe^{3+} and then decreased the photocatalytic activity. Thus, another indirect electron transfer to the Fe^{3+} through the doped level is important for the high performance of the Fe/TiO_2 based photocatalyst.

3.2. *The effect of electron donor or acceptor states of doped metal ions*

To clarify which indirect electron transfer to the Fe^{3+} through electron excitation, from the doped level to conduction band or from valence band to the doped level, as illustrated in Fig. 4, we examined the effect of codoping effect of Rh and Sb into the TiO_2 lattice because in the case of Rh alone doping, Rh^{4+} forms acceptor level in the TiO_2 bandgap and in the case of codoping with Sb^{5+}, Rh^{3+} which is formed by reduction of Rh^{4+} by charge compensation forms donor level.

Fig. 5 shows UV–vis diffuse reflectance spectra of Rh doped TiO_2 (Rh:TiO_2), Rh–Sb codoped TiO_2 (Rh–Sb:TiO_2) in which Sb was codoped at the ratio of Sb/Rh = 1, and Rh–2Sb codoped TiO_2 (Rh–2Sb:TiO_2) in which Sb was codoped at the ratio of Sb/Rh = 2. For the Rh–Sb:TiO_2 and Rh–2Sb:TiO_2, the absorption rates at the range $\lambda = 500$–700 nm were decreased compared to that of the Rh:TiO_2, indicating that Rh^{4+} turned Rh^{3+} by codoping with Sb. Therefore, for the Rh–Sb:TiO_2 and Rh–2Sb:TiO_2, the donor level due to Rh^{3+} would be introduced. Based on the previous report, at the ratio of Sb/Rh = 1 the Rh^{4+} remained and then at Sb/Rh = 2 all the Rh^{4+} turn Rh^{3+}. Also in this present work, the absorption rate at the range of $\lambda = 500$–700 nm of the Rh–2Sb:TiO_2 was further decreased compared to the Rh–Sb:TiO_2, indicating that for the Rh–2Sb:TiO_2 more Rh^{3+} of donor state were introduced then the Rh–Sb:TiO_2. In contrast, for the Rh:TiO_2, Rh^{4+} would be formed

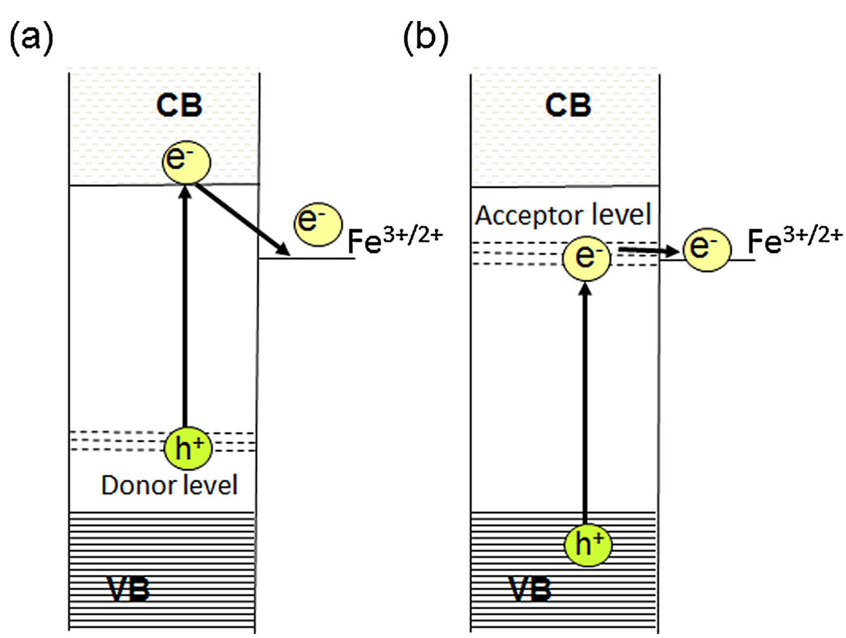

Fig. 4. Indirect electron transfer paths to the Fe^{3+} via (a) donor level and (b) acceptor level.

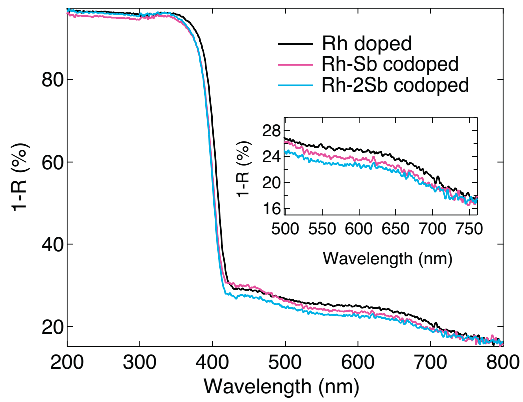

Fig. 5. UV–vis diffuse reflectance spectra of $Rh:TiO_2$, $Rh–Sb:TiO_2$ and $Rh–2Sb:TiO_2$.

an acceptor level. The effect of states for doped metal ions on the photocatalytic activity under visible light irradiation of $\lambda = 470$ nm is shown in Fig. 6. Before the grafting of Fe^{3+}, both photocatalysts of the $Rh:TiO_2$ and $Rh–Sb:TiO_2$ showed slight photocatalytic activities. The photocatalytic activity of the $Rh:TiO_2$ was a little higher than that of the $Rh–Sb:TiO_2$. Oxidation of acetaldehyde were induced at TiO_2 valence band for the $Rh:TiO_2$, while at donor level due to Rh^{3+} for the $Rh–Sb:TiO_2$. Since the redox potential of doped level is more negative than that of TiO_2 valence band, the oxidative ability of the $Rh–Sb:TiO_2$ was weaker than that of the $Rh:TiO_2$. In addition, since the mobility of holes at the doped level may be significantly small than that of valence band holes, the photocatalytic activity was small. Therefore, the decrease of the photocatalytic activity by codoping with Sb would be due to the weaker oxidative ability and poor continuousness of the donor level of doped Rh^{3+}.

After the grafting of Fe^{3+}, their photocatalytic activities were enhanced and higher than the Fe/TiO_2 in which TiO_2 was non-doped. This indicates that the indirect electron transfer to the Fe^{3+} via the doped Rh species contributed to the photocatalytic activity in addition to the direct electron transfer to the Fe^{3+} which occurred also in the Fe/TiO_2. Compared to the codoped photocatalysts of Rh and Sb with the $Fe/Rh:TiO_2$, the photocatalytic activities became lower as Sb content increased. Before and after the grafting of Fe^{3+}, the generation rate of CO_2 by decomposition of

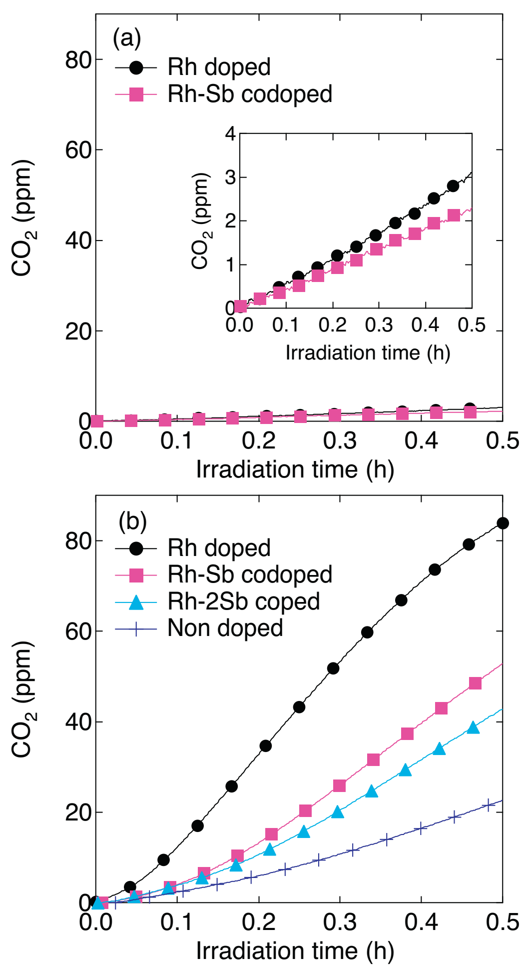

Fig. 6. Time profiles of CO_2 generated by photocatalytic decomposition of gaseous acetaldehyde on the photocatalysts under visible light irradiation ($\lambda = 470$ nm) (a) before and (b) after grafting of Fe^{3+}.

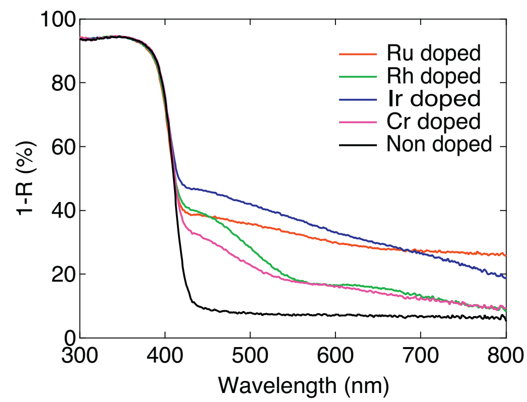

Fig. 7. UV–vis diffuse reflectance spectra of the $Me:TiO_2$.

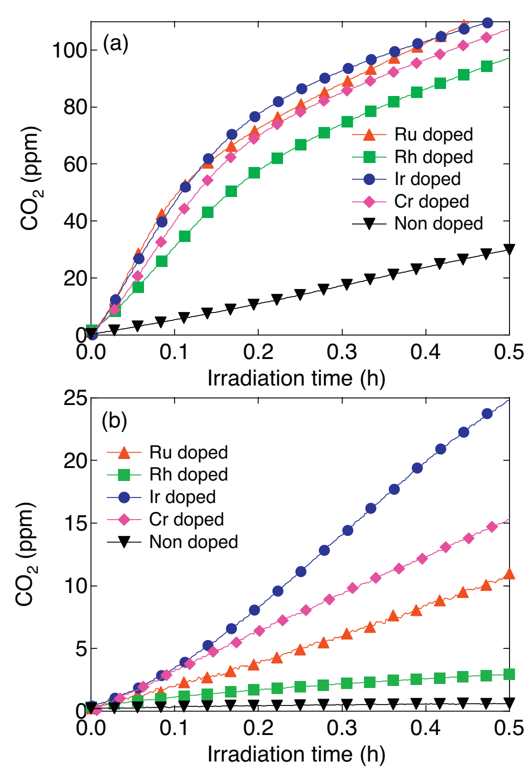

Fig. 8. Time profiles of CO_2 generated by photocatalytic decomposition of gaseous acetaldehyde on the $Fe/Me:TiO_2$ under visible light irradiation of (a) $\lambda = 470$ nm and (b) $\lambda = 625$ nm.

acetaldehyde were increased about 31 times and 21 times for the Rh:TiO_2, and the Rh–Sb:TiO_2, respectively. This indicates that the indirect electron transfer via donor level (Fig. 4(a)) was less effective than that via acceptor level (Fig. 4(b)). However, since the photocatalytic activities of the codoped photocatalysts were higher than the Fe/TiO_2, the indirect electron transfer via donor level contributed to the photocatalytic activity to some extent. Therefore, it is important for the photocatalytic activity of Fe/TiO_2 based photocatalyst to dope metal ions which form an electron acceptor in TiO_2 bandgap.

These results showed the different tendency from the previous report [11]. The photocatalytic activity for evolution of O_2 by water oxidation in the presence of silver nitrate under visible light irradiation appeared by codoping of Rh and Sb and the photocatalytic activity was the highest at the ratio of Sb/Rh = 2. In its system, the acceptor level due to Rh^{4+} was not high enough to reduce Ag ion, resulting in the poor activity for water oxidation. In contrast, for the Fe/TiO_2 based photocatalyst, the reduction of O_2 into H_2O_2 via two electron process occur at the Fe^{3+} site. Therefore, the decrease of redox potential of the acceptor level did not affect the photocatalytic activity for gaseous acetaldehyde because electrons at valence band transfer to the Fe^{3+} via acceptor level as shown in Fig. 4(b).

3.3. The effects of redox potentials of various doped metal ions

To examine the effects of redox potentials of doped metal ions on the photocatalytic performance, Ru, Rh, Ir and Cr ions were doped in the TiO_2. Fig. 7 shows UV–vis diffuse reflectance spectra of the metal ion doped TiO_2 (Me:TiO_2). For all the Me:TiO_2, new absorptions appeared at visible light region of longer wavelength than absorption edge of TiO_2. The new absorption would be mainly due to the electron excitation between TiO_2 valence band or conduction band, and doped metal ions. For the Rh:TiO_2 and Cr:TiO_2, the relatively large new absorptions extended to about $\lambda = 550$ nm and relatively small new absorptions extended to about $\lambda = 800$ nm. For the Ru:TiO_2 and Ir:TiO_2, the new absorptions were relatively large over wide visible light region. Based on these absorption wavelength, Rh and Cr ions seem to be formed their doped level at upper or bottom parts in the bandgap and Ru and Ir ions seem to be formed their doped level at middle part in the bandgap.

Fig. 8 show time profiles of CO_2 amounts generated by decomposition of gaseous acetaldehyde under visible light irradiation of $\lambda = 470$ nm and 625 nm after grafting of Fe^{3+}. Under visible light irradiation of $\lambda = 470$ nm, the Fe/Me:TiO_2 showed all higher CO_2 generation rates than the Fe/TiO_2. Among the Fe/Me:TiO_2 photocatalysts, there was no significant difference in their

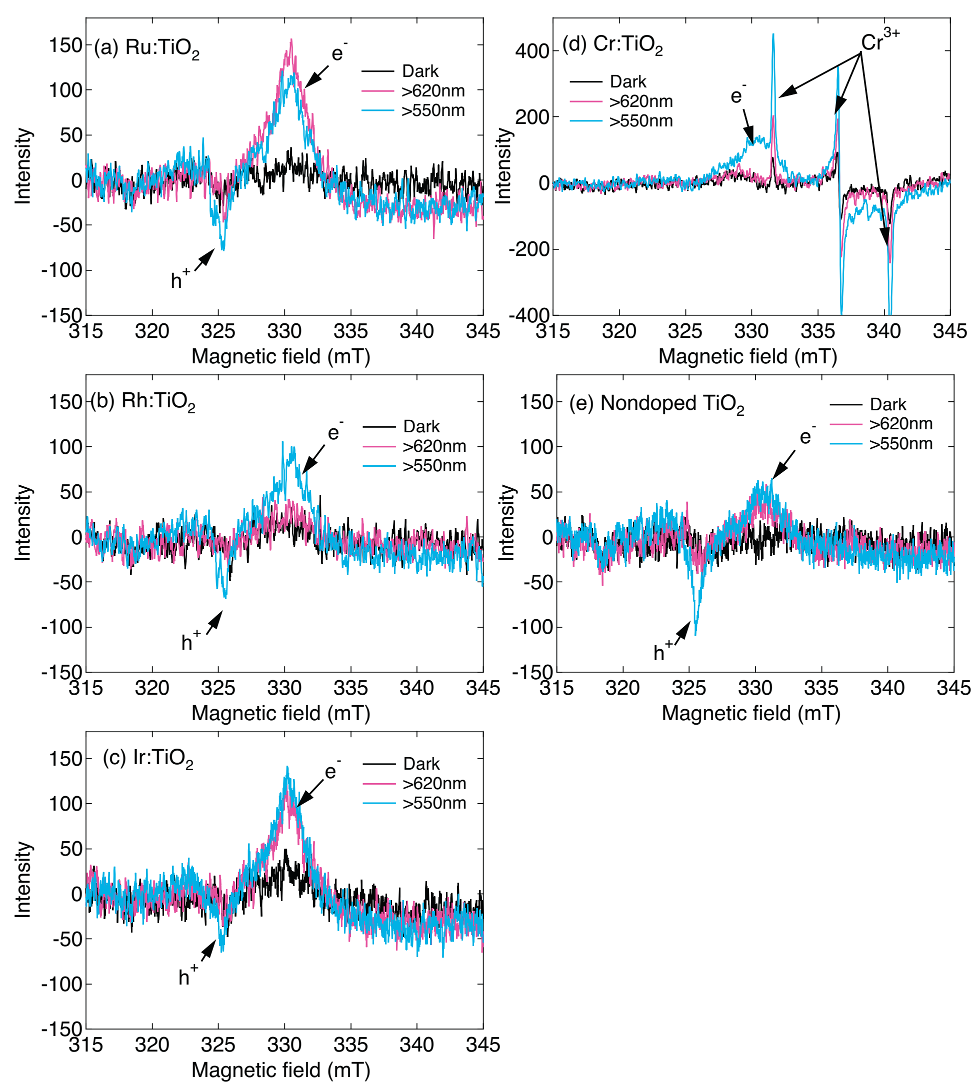

Fig. 9. ESR spectra of (a) Ru:TiO_2, (b) Rh:TiO_2, (c) Ir:TiO_2, (d) Cr:TiO_2 and (e) TiO_2.

photocatalytic activity on 470 nm irradiation. Moreover, complete decomposition of acetaldehyde achieved after about 6 h for the Fe/Me:TiO_2 photocatalyst, while for the Fe/TiO_2 photocatalyst it achieved after over 16 h. Then under visible light irradiation of $\lambda = 625$ nm, the Fe/TiO_2 showed no detectable amount of CO_2. In contrast, the Fe/Me:TiO_2 showed all photocatalytic decomposition ability. Especially, the Fe/Ir:TiO_2 and Fe/Cr:TiO_2 had high photocatalytic activities. From these results, the suitable dopants for response of longer-wavelength visible light were Ir > Cr > Ru > Rh in order.

Fig. 9 shows ESR spectra of the Me:TiO_2 under dark and light irradiation at 77 K. The Cr:TiO_2 shows ESR signals of $g_1 = 1.961$, $g_2 = 1.931$ and $g_3 = 1.911$ even under dark condition. The signals would be assigned to Cr^{3+}. Considering its ionic radii compared to Ti^{4+} whose ionic radius is 0.605 Å, Cr^{3+} was reasonable as doped state because its ionic radius is 0.615 Å. Based on a previous report, Cr^{3+} played a role as donor [19]. However, under light irradiation, the signals assigned to Cr^{3+} increased. This indicates that Cr species of higher valence such as Cr^{4+} coexisted with Cr^{3+} and then by light irradiation Cr species of higher valence received electrons to become Cr^{3+}. Thus, Cr species of higher valence played a role as acceptor and Cr^{3+} would not played a role as donor to a large extent in this work.

Next, we focused on the generation behavior of electrons and holes for the Me:TiO_2. In the case of visible light irradiation of $\lambda > 620$ nm, the Rh:TiO_2 and Cr:TiO_2 showed no ESR signals. In contrast, the Ru:TiO_2 and Ir:TiO_2 showed the ESR signals assigned to electron trapped as Ti^{3+} ($g = 1.97$), whose intensity was clearly large compared to the nondoped TiO_2. This indicated that electron excitation frequently occurred in the Ru:TiO_2 and Ir:TiO_2. This active electron excitation would be concerned with the defect level because by doping metal ions structural defects such as oxygen vacancy were introduced. Considering their ionic radii compared to Ti^{4+}, Ru, Ir and Rh seem to be doped as tetravalent because their ionic radii are 0.620, 0.625 and 0.600 Å, respectively. Cr was doped as mixed valence of trivalent and higher valence as mentioned above. Ru^{4+} and Ir^{4+} are relatively large in ionic radius compared to Rh^{4+} and Cr^{3+} and Cr^{4+}. By doping of relatively large Ru^{4+} and Ir^{4+}, a large amount of structural defects introduced in the TiO_2 host, leading to the active electron excitation under visible light irradiation of $\lambda > 620$ nm.

Fig. 10(a) shows the amounts of O_2^- generated on the Me:TiO_2 under light irradiation of $\lambda \equiv 625$ nm. The electrons having a potential energy of +0.38 V (vs. SHE at pH = 0) can reduce O_2 into O_2^- at the experimental condition [20]. Therefore, by measuring the amount of O_2^-, the redox potential of dopants can be examined. To detect O_2^- generated by one-electron reduction of O_2 other than generated by oxidation of H_2O_2, light irradiation time was fixed at 1 s. For the non-doped TiO_2, the generation amount of O_2^- was larger than that of the Me:TiO_2. For the non-doped TiO_2, O_2 was reduced to O_2^- by an electron excited at conduction band from defect level under the light irradiation of $\lambda \equiv 625$ nm. This result indicated that all kinds of dopant used played a role as acceptor because if they play a role as donor, the generation amount of O_2^- should increase due to electron excitations from dopants to conduction band. Among the Me:TiO_2, the generation amount of O_2^- was decreased in the order of Rh > Cr > Ru > Ir. This order was opposite tendency to the ESR results. Based on the ESR spectra, under light irradiation of $\lambda > 620$ nm, the signals due to electrons trapped at Ti^{3+} were observed only for the Ru:TiO_2 and Ir:TiO_2. This indicated that for Me:TiO_2, O_2^- was generated by dopants rather than electrons excited at conduction band. Since the order of the redox level of dopants should be consistent with that of the O_2^- amount, their redox levels would be more negative in the order of Rh > Cr > Ru > Ir as illustrated in Fig. 11. This order was in good agreement with their absorption spectra.

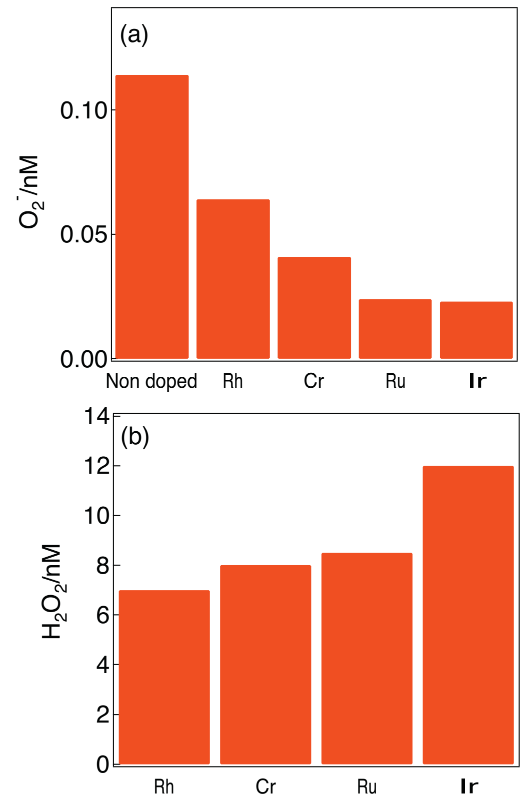

Fig. 10. (a) Amounts of O_2^- generated on the Me:TiO_2 and (b) amounts of H_2O_2 on the Fe/Me:TiO_2 under visible light irradiation ($\lambda = 625$ nm).

Next, Fig. 10(b) shows the amounts of H_2O_2 after grafting Fe^{3+} under light irradiation of $\lambda \equiv 625$ nm to determine the degree of electron transfer to the Fe^{3+} from the dopants. The electrons having a potential energy of +0.695 V (vs SHE at pH = 0) can reduce O_2 into H_2O_2 by two-electron process [20]. Based on the

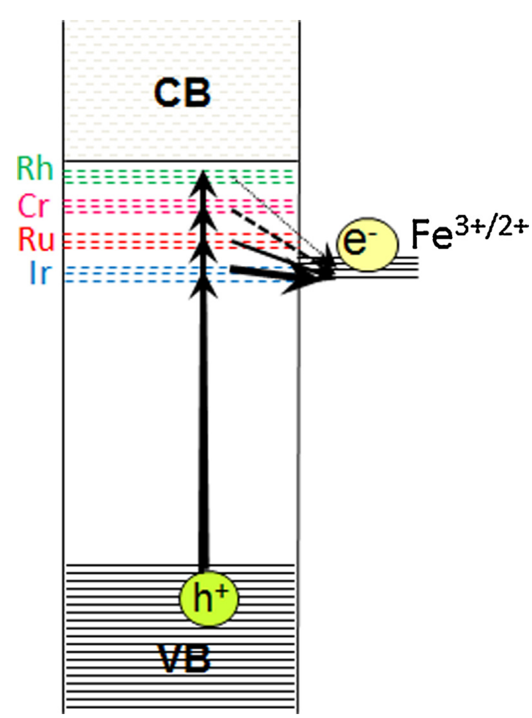

Fig. 11. Schematic energy level diagram for the Fe/Me:TiO_2.

previous report [10], the redox potential of the grafted Fe^{3+} to Fe^{2+} was at or less positive than +0.695 V (vs SHE at pH = 0) because H_2O_2 was dominantly generated compared to O_2^- for Fe/TiO_2. To detect H_2O_2 generated by two-electron reduction of O_2 other than by one-electron reduction of O_2^-, light irradiation time was fixed at 3 s. The generation amount of H_2O_2 was decreased in the order of Ir > Ru > Cr > Rh. This generation tendency of H_2O_2 was opposite to that of O_2^-. Through the dopant with more positive redox potential, electron can transfer more easily to the Fe^{3+} as illustrated in Fig. 11. It was considered that this was due to the small energy loss of electrons when the redox potential of dopant was close to that of the Fe^{3+}. Therefore, it was concluded that the high photocatalytic activity of the Fe/Ir:TiO_2 under visible light irradiation was attributable to the acceptor level due to Ir^{4+} formed close to the redox potential of the grafted Fe^{3+}. The photocatalytic activity of the Fe/Ru:TiO_2 seemed to be somewhat lower compared to the Fe/Cr:TiO_2 although the acceptor level due to Ru^{4+} formed closer to the grafted Fe^{3+}. We consider that this was resulted from the larger amount of structural defects introduced by doping Ru^{4+} as mentioned at the ESR measurements (Fig. 9). Since the structural defect lower the photocatalytic activity, the photocatalytic activity of the Fe/Ru:TiO_2 was lower than that of the Fe/Cr:TiO_2 in which a large amount of structural defects were not introduced. Thus, by doping metal ions which formed an acceptor level, the photocatalytic activity was enhanced and simultaneously structural defects which lowered the photocatalytic activity were introduced. The visible-light driven performance of Fe/TiO_2 photocatalyst was determined by competition of electron transfer to the Fe^{3+} via acceptor level and recombination of hole–electron at the structural defect.

4. Conclusions

We examined dominated factors for visible-light driven performance of the Fe/TiO_2 based photocatalyst. The two-step electron excitation from valence band to conduction band via defect level under visible light irradiation could not contribute to the photocatalytic activity and decreased the efficiency of the direct electron transfer from valence band to the Fe^{3+}, resulting in decrease of photocatalytic activity. Therefore, by doping meal ions the indirect electron transfer via doped metal ions to the Fe^{3+} was important for the performance. Furthermore, the indirect electron transfer effectively occurred via the acceptor state rather than the donor state of metal ions, which leaded to enhancement of the photocatalytic activity. Especially, it was important that acceptor level close to the redox potential of the grafted Fe^{3+} to Fe^{2+} was formed by doping metal ions, because indirect electron transfer from valence band to the Fe^{3+} via the acceptor level easily occurred.

References

[1] A. Fujishima, X. Zhang, D. Tryk, Surf. Sci. Rep. 63 (2008) 515–582.
[2] M.A. Henderson, Surf. Sci. Rep. 66 (2011) 185–297.
[3] M. Anpo, P.V. Kamat (Eds.), Environmentally Benign Photocatalysis Application of Titanium Dioxide based Materials, Springer, New York, 2010.
[4] R. Asahi, T. Morikawa, T. Ohwaki, K. Aoki, Y. Taga, Science 293 (2001) 269–271.
[5] T. Umebayashi, T. Yamaki, H. Ito, K. Asahi, Appl. Phys. Lett. 81 (2002) 454–456.
[6] J. Zhu, J. Ren, Y. Huo, Z. Bian, H. Li, J. Phys. Chem. C 111 (2007) 18965–18969.
[7] Y. Ishibai, J. Sato, S. Akita, T. Nishikawa, S. Miyagishi, J. Photochem. Photobiol. A 188 (2007) 106–111.
[8] H. Irie, K. Kamiya, T. Shibanuma, S. Miura, D.A. Tryk, T. Yokoyama, K. Hashimoto, J. Phys. Chem. C 113 (2009) 10761–10766.
[9] H. Yu, H. Irie, Y. Shimodaira, Y. Hosogi, Y. Kuroda, M. Miyauchi, K. Hashimoto, J. Phys. Chem. C 114 (2010) 16481–16487.
[10] M. Nishikawa, Y. Mitani, Y. Nosaka, J. Phys. Chem. C 116 (2012) 14900–14907.
[11] R. Niishiro, R. Konta, H. Kato, W.J. Chun, K. Asakura, A. Kudo, J. Phys. Chem. C 111 (2007) 17420–17426.
[12] F.E. Oropeza, R.G. Egdell, Chem. Phys. Lett. 515 (2011) 249–253.
[13] R. Konta, T. Ishii, H. Kato, A. Kudo, J. Phys. Chem. B 108 (2004) 8992–8995.
[14] S. Kawasaki, K. Akagi, K. Nakatsuji, S. Yamamoto, I. Matsuda, Y. Harada, J. Yoshinobu, F. Komori, R. Takahashi, M. Lippmaa, C. Sakai, H. Niwa, M. Oshima, K. Iwashina, A. Kudo, J. Phys. Chem. C 116 (2012) 24445–24448.
[15] T. Hirakawa, Y. Nosaka, J. Phys. Chem. C 112 (2008) 15818–15823.
[16] Y. Nakaoka, Y. Nosaka, J. Photochem. Photobiol. A 110 (1997) 299–305.
[17] J.M. Coronada, A.J. Maira, J.C. Conesa, K.L. Yeung, V. Augugliaro, J. Soria, Langmuir 17 (2001) 5368–5374.
[18] C. Di Valentin, G. Pacchioni, A. Selloni, J. Phys. Chem. C 113 (2009) 20543–20552.
[19] D. Wang, J. Ye, T. Kako, T. Kimura, J. Phys. Chem. B 110 (2006) 15824–15830.
[20] Y. Nosaka, S. Takahashi, H. Sakamoto, A.Y. Nosaka, J. Phys. Chem. C 115 (2011) 21283–21290.